SPACE TELESCOPE
European Coordinating Facility

ST-ECF Instrument Science Report NGST 2002-01

Pixels, slits and facets for a MEMS-type spectrograph for NGST

Santiago Arribas, Peter Jakobsen, Robert Fosbury & Wolfram Freudling

Pixels, slits, and facets for a MEMS-type spectrograph for NGST

S. Arribas (STScI), P. Jakobsen (ESTEC), R.A.E. Fosbury (ST-ECF) and W. Freudling (ST-ECF)

V2.6 February 2002

Abstract

This report addresses the question of the choice of MEMS and detector element (facet and pixel respectively) sizes for the NGST near-infrared multi-object spectrograph NIRSpec. Using a specially modified spectroscopic exposure time calculator, we address both the 'efficiency' of observing single sources and the 'speed' of observing a field of sources with a space density typical for galaxies near the NGST magnitude limit. Because of the different relative importance of sky and detector noise sources, the conclusions differ somewhat between spectral resolutions of R = 1000 and R = 100. We believe, however, that a reasonable compromise can be reached by using a detector pixel scale close to 0.1 arcsec/pixel. A rectangular facet — with the long dimension perpendicular to the dispersion — is preferred. This analysis assumes an ideal generic MEMS device (MSA or MMA). The actual properties of the selected MEMS device, the detector performance and the achievable PSF may require some future refinement of this analysis.

1. Introduction

In the baseline concept for the NGST-NIR spectrograph (NIRSpec), a MEMS array is used to create the focal plane slit masks necessary for multi-object spectroscopy. When a unit of the MEMS array (hereafter, facet) is *on*, the corresponding portion of the sky is selected and imaged (through the spectrograph) onto the detector array at the focal plane of the camera.

In this note, we discuss how the pixel scale at the detector and the slit dimensions (width and length — usually defined by more than one facet) affect the performance of NIRSpec.

The discussion requires the analysis of the different sources of noise (zodiacal light, detector dark current and readout, etc) and how they combine in the different designs. The principal tool required for this analysis is an Exposure Time Calculator (ETC). The most complete NGST–ETC is included in NMS (NGST Mission Simulator: Samsom & Petro, 2000). However, this code does not include the slit effects which are important for our discussion.

Therefore, as a first step we have developed a new ETC optimised for spectroscopy (Spectroscopic ETC; hereafter S–ETC) which takes into account the slit effects (i.e., slit losses; changes in the zodiacal light) and updates other relevant issues (Section 2). In Section 3 we discuss the application of a useful *figure of merit*. In Section 4 we discuss how the sensitivity of the spectrograph changes for different choices of slits and pixels. In Section 5

the global efficiency, or 'speed', for multi-object observations is analysed as a function of the pixel scale. In Section 6 we comment on the implications for the facet geometry and size. Finally, in Section 7 we outline our main conclusions.

A 6.5m aperture telescope diffraction limited at 2μm is assumed throughout. Two spectral resolutions (R = 100 and 1000) are discussed. DRM15 (Deep spectroscopic survey); see http://www.stsci.edu/ngst/science/drm/
is considered to be the science program driving the NIRSpec design.

2. Spectroscopic ETC

The main assumptions in the S–ETC are:

- ❏ We use a PSF based on the simulations generated by Bely et al. (2001, NGST-Monograph No. 7), transformed for our 6.5m telescope. For the present calculations we have selected a PSF with low-frecuency errors of 0.144μm (rms) in wavefront and the same mid-frequency errors as HST. This PSF just fulfills the optical requirements for the OTA as established by Bely et al.
- ❏ The Zodiacal background is based on the revised COBE data by Giavalisco et al (2001, private communication).
- ❏ Slit losses are calculated assuming the above PSF (point sources). Changes in the zodiacal contribution to the noise depending on the slit width, are taken into account.
- ❏ For long exposures (DRM15), the dark current is assumed to be the major contributor to the detector noise. A value of 0.02 e^-/s is assumed.
- ❏ For the NIRSpec, the details of the applied spectrum extraction techniques are relevant since the wings of the PSF will carry a relatively important fraction of the flux. S–ETC uses both the standard extraction procedure (no weights), and the 'optimal extraction' method (weights based on the variance: Horne, 1988). The successful application of these techniques depends on a detailed knowledge of the background, the detector noise and the optical distortions of the spectrograph. For the results presented here, it is assumed that these are known.
- ❏ Simulations varying the location of the object relative to the detector pixel array given that the latter may undersample the PSF. The numbers presented here are the result of averaging several different object locations.

3. Figure of merit

The ASWG ranked *ultimate sensitivity* as the first priority for the NGST instrumentation. In the particular case of NIRSpec, since the high redshift galaxies in DRM15 will be barely resolved, sensitivity is favoured over spatial resolution.

However, for multi-object observations, the performance of the spectrograph will be measured by its speed observing 'interesting' galaxies (at the required S/N) per unit observing time.

Initially, we look for the pixel scale (and slit width) that maximises sensitivity. Later we analyse the speed of the spectrograph as a function of the pixel scale.

4. Sensitivity = F(pixel scale, slit)

4.1 Case for slit width = 2 pixels

R = 1000

Initially we consider the standard assumption that the slit width (not the facet size) is sampled by two detector pixels.

Using S-ETC we have generated Figure 1 (top) showing the S/N obtained in an arbitrary observing time as a function of the detector pixel size†. Further assumptions are indicated in the figure.

The conclusion from this is clear: if the slit is sampled by two detector pixels, a scale of about 0.16 arcsec/pixel maximises the S/N for a single observation, under the assumptions mentioned above. However, this selection is not critical, and values in the range 0.14–0.20 arcsec/pixel give essentially the same results.

Using a similar methodology for a 8m telescope, Petro & Stockman (2000) found that a value of 0.11 arcsec/pixel maximises S/N (minimises exposure) for the NIR spectrograph. Taking into account the scaling with aperture, both analyses agree.

To better understand the behavior shown in Figure 1 (top), the other two panels illustrate how the signal (middle panel) and the noise (bottom panel) change with the pixel size. The behavior of the signal clear: larger detector pixels imply a larger slit and hence fewer slit losses.

In the bottom panel, the total noise as well as its breakdown into the individual noise sources is represented. The poissonian noise is clearly related to the signal from the source. The zodiacal light increases with the slit width. Detector noise is more important for smaller pixels, because this requires a larger number of pixels to cover the object along the slit (i.e., across the spectral direction). Note, however, that the zodiacal and detector noises do not show a linear behaviour with the number of pixels due to the pixel weighting applied in the optimal spectral extraction.

R = 100

In Figure 2 we present similar panels for the case R = 100. Because in this case the zodiacal light is relatively much more important, the advantage of having a small number of pixels (large pixel scale) is offset by the increase in zodiacal background due to the larger input slit.

The conclusion here is that in the case where the slit is sampled by two detector pixels, a scale of 0.085 arcsec/pixel maximises the S/N for a single observation, under the assumptions mentioned above. However, values in the range 0.07–0.12 arcsec/pixel give essentially similar results.

Dependence on the assumptions

How will the result inferred from Figures 1 & 2 change under other assumptions?

† Strictly speaking we are representing S/N/√t as a function of the pixel size. However, the factor √t has no relevance in the present discussion since it does not affect the shape of the curve.

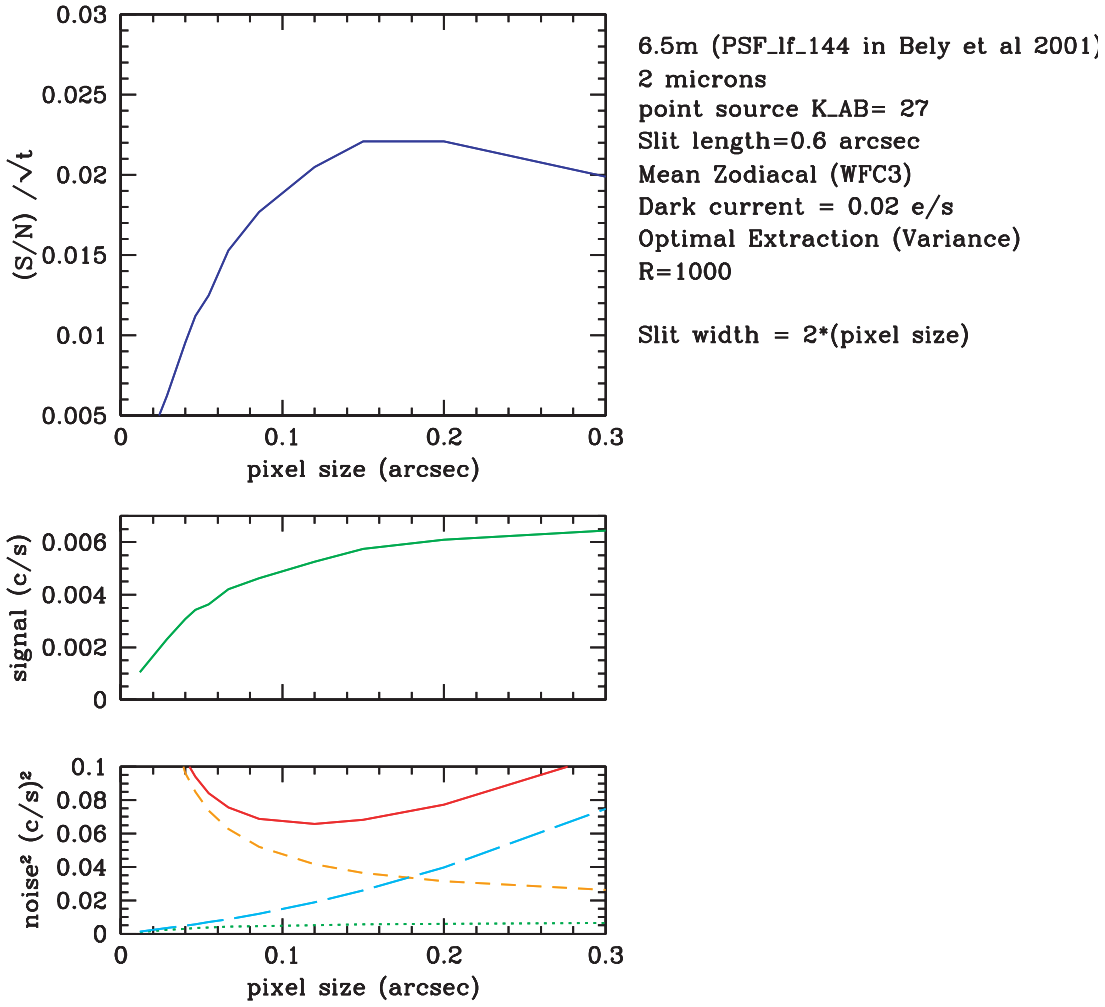

Figure 1: *top: S/N (per √t) as a function of the detector pixel size (slit sampled by 2 detector pixels), for R = 1000. Other assumptions are indicated in the upper right corner. Middle: variation of the signal with the pixel size. Bottom: variation of the noise with the pixel size; dotted line – poissonian from the source; small dashes – detector; large dashes – zodiacal light; continuous line – all noise sources combined.*

Wavelength: for longer wavelengths, larger pixels are needed to maximise S/N. As a first approach a linear behaviour with wavelength can be considered.

Background: for a smaller zodiacal background, larger pixels are needed to maximise S/N — and vice versa.

Dark current: for a dark current larger than the one considered (0.02 e/s), the pixel scale should be somewhat larger.

Extraction: for a standard extraction method (no weights), the detector and zodiacal noises are more important for small pixel sizes and, therefore, a larger pixel scale is needed.

Object size: for extended objects, the pixel scale should be larger. (Note that we are optimising sensitivity, not resolution).

4.2 Case for slit width ≠ 2 pixels: effects of the slit width

High redshift galaxies near the magnitude limit of NIRSpec are expected to be barely re-

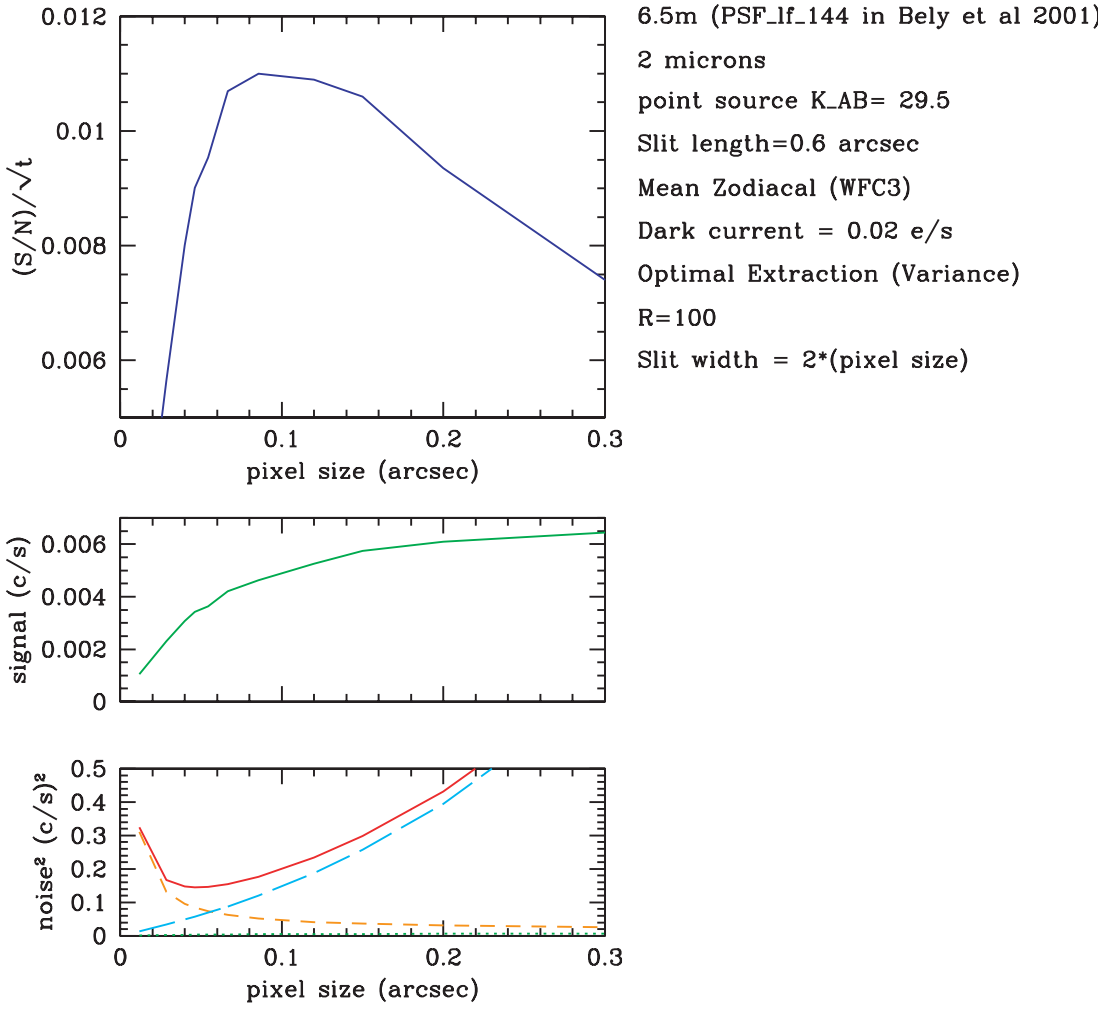

Figure 2: *The same calculation for R = 100.*

solved with typical half-light radii of 0.1–0.15 arcsec (Gardner et al. 2000; Pirzkal et al. 2001). Under these circumstances, large slit widths (≥ 0.4 arcsec) imply a greater signal because light contained in the wings of the PSF is included and result in only a modest loss in spectral resolution which is determined largely by the object size. Larger slit widths do imply, however, a greater zodiacal noise. Since observations at R = 1000 and R = 100 occur in very different regimes, i.e., *detector limited* and *zodiacal limited* respectively, the effects of the slit width are different in both cases.

In this subsection we analyse the case in which the slit width and the pixel are not coupled.

R = 1000

Using S–ETC we have generated Figure 3 which shows S/N vs. pixel size curves considering three fixed values for the slit widths (0.3, 0.45, 0.6 arcsec).

We can see that relatively large slit widths (~ 0.3–0.45 arcsec) give the highest sensitivity, with pixel scales in the range 0.12–0.2 arcsec/pix. [*Note that these sensitivities are larger than the case where the slit is sampled by exactly two pixels for both small pixel scales (because the slit collects more light from the object) and large pixel scales (because the background noise is smaller)*].

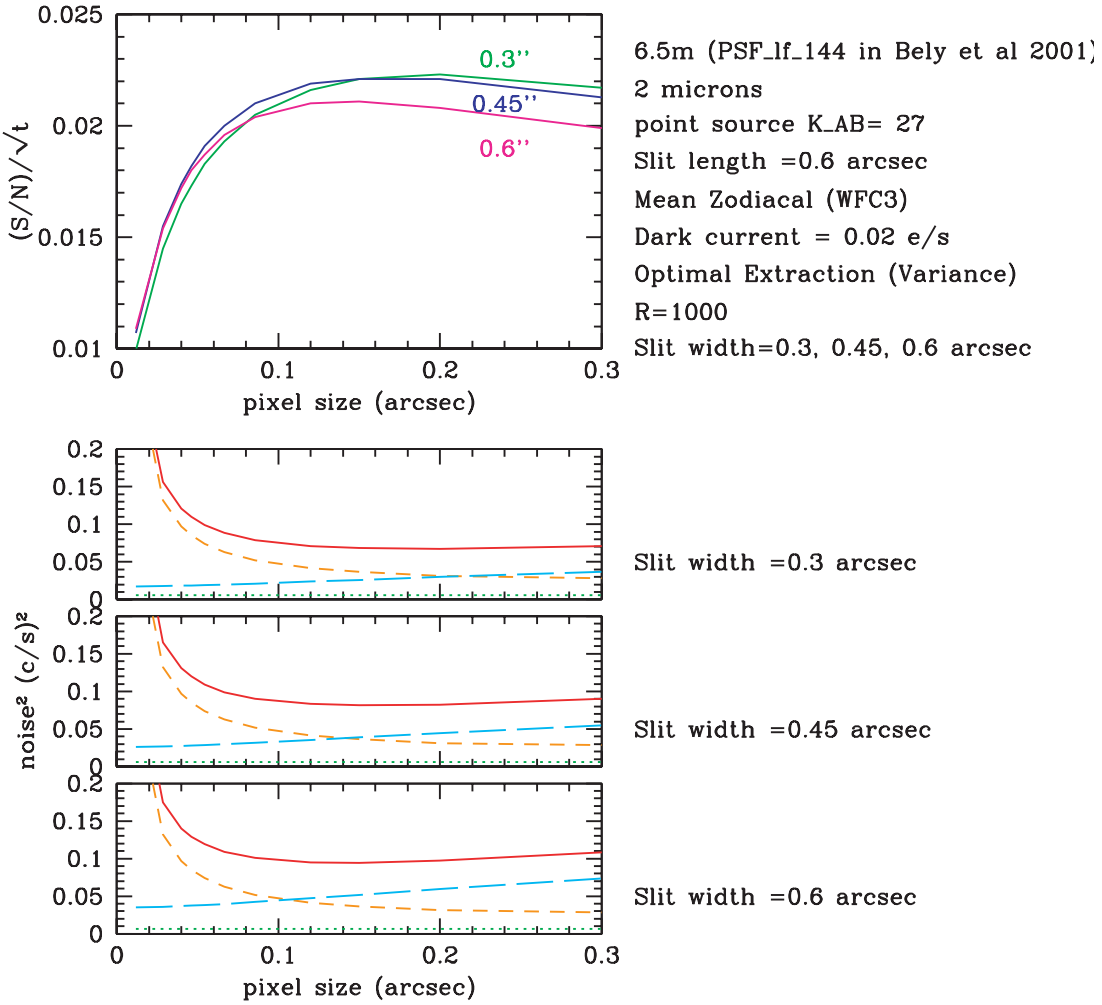

Figure 3: *S/N (per √t) as a function of the detector pixel scale for three slit widths (0.3, 0.45, 0.6 arcsec) and R = 1000. Other assumptions are indicated in the Figure. Lower panels show the relative importance of the different noise sources for the three slits; dotted line – poissonian from the source; small dashes – detector; large dashes – zodiacal; continuous line - all noise sources combined.*

The reason for the relatively large slit widths inferred from Figure 3 can be understood as follows. When we are observing point sources in a *detector limited* regime, the use of relatively large slit width implies a net gain of signal (flux in the wings of the PSF), while the negative effects due to the increase in zodiacal light are less relevant.

According to Figure 3, for slits ~ 0.3–0.45 arcsec, a scale of 0.1 arcsec/pixel implies only a moderate loss in S/N (~ 5%) with respect to the maximum, but it may have other advantages (see below). At a scale of 0.05 arcsec the loss is more serious (~20% in S/N). In addition, the results for small pixel scales depend more on the extraction techniques which, in practice, are subject to uncertainties not considered here (Section 2).

R = 100

In Figure 4 we present the S/N vs. pixel scale for R = 100, and three fixed values for the slit width (0.1, 0.2, 0.3 arcsec). Since in this case the observations are *zodiacal light limited*, relatively large slits have a serious impact on the S/N. Optimum values are obtained for slit widths in the range 0.2–0.3 arcsec, with a pixel scale in the range 0.05–0.1 arcsec/pixel.

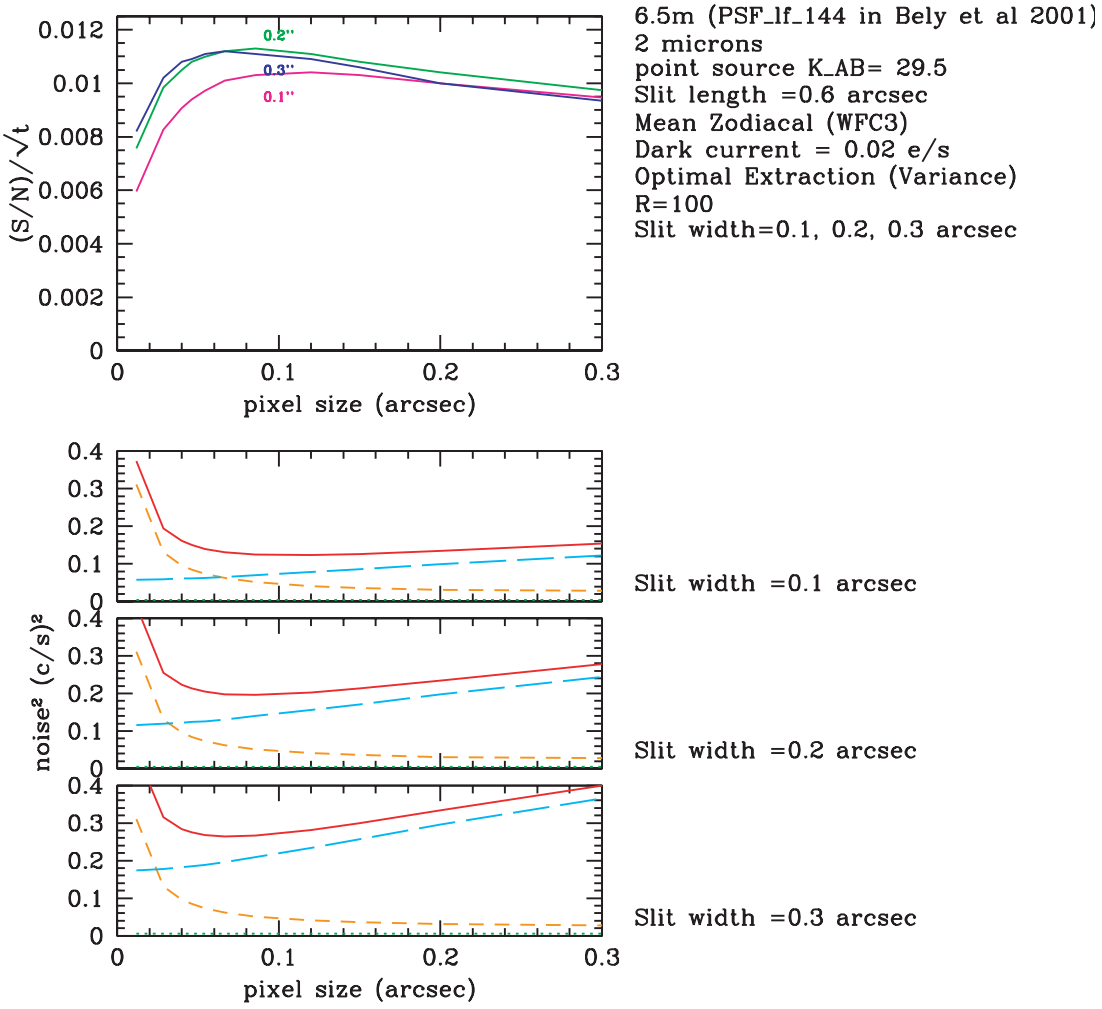

Figure 4: *S/N (per √t) as a function of the detector pixel scale for three slit widths (0.1, 0.2, 0.3 arcsec), and R = 100. Otherwise as for previous Figure.*

5. Speed = F(pixel scale, slit)

Slit length: effects on multi-object observations

The effects of the slit width have been analysed in the previous section. Extending the slit length beyond the dimensions of the object has no effect on the source signal but it does allow better local background determination. For a multi-object pattern, however, the longer slit exacerbates crowding effects.

Due to the fact that observations at R = 1000 and at R = 100 are affected differently by the noise sources, different strategies need to be employed to minimise crowding effects in the two cases.

In Figure 5 we illustrate the impact on the required observing time when the background is increased by factors of 2 and 3 (which simulates the overlapping of 2 and 3 spectra, respectively), as a function of the pixel scale. There are two main conclusions from this figure:

1. an increase in the background light is less relevant for R = 1000 than for R = 100.

2. an increase in background light is less relevant for small pixel scales since, for them, the detector noise is more important.

Therefore, smaller pixel scales and higher spectral resolution minimise the effects of overlapping spectra.

When two or more spectra overlap on the detector, the increase in noise (mainly due to the

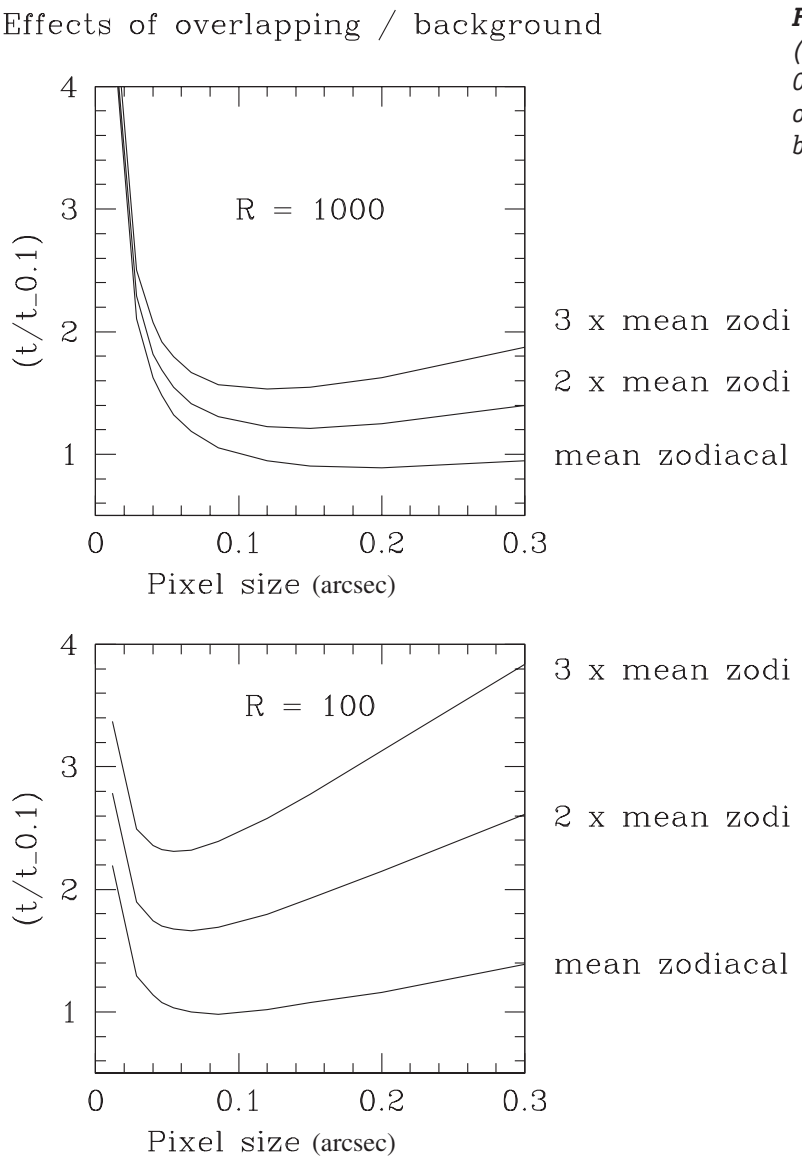

Figure 5: *Exposure time required (normalized to the one for a scale of 0.1 arcsec/pixel, mean background) for one, two, and three times the mean background for R = 1000 and R = 100.*

zodiacal background in DRM15-like observations) makes it necessary to employ longer integrations to reach a given S/N. What is the trade-off between multiplexing gain and integration time for this situation? How does it depend on spectral resolution and/or on the selected pixel scale? The detailed modeling of the multiplexing gain and sensitivity as a function of the pixel scale and slit dimensions is complex, e.g., zodiacal light depends on both wavelength and source position and the crowding requires Monte-Carlo simulations. It also depends on the density of objects and the type of observations (continuum/emission line) and on the particular geometry of the detector/MEMS, etc.

For the present discussion we will assume some reference values based on previous simulations for the crowding for a density of 100 objects/arcmin^2. In particular we will consider that for R = 1000, 31%, 56%, and 74% of the galaxies in the focal plane can be

observed in 1, 2 and 3 exposures without allowing overlap. For R = 100, 45%, 65%,and 80%, can be selected in 1, 2 and 3 exposures respectively. These values can be significantly different in practice, but they give us a reference for the present discusion and it avoids the need for the detailed specification of parameters.

In Figure 6, we represent the 'speed' of the spectrograph as a function of the pixel scale for R = 1000 and R = 100 in three situations: (i) no overlap allowed, (ii) overlap of two spectra is allowed and (iii) overlap of three spectra is allowed. The required exposure times have been set to reach the required S/N in the most unfavourable case. The speeds are normalised to the value corresponding to 'no overlap' for scale = 0.10 arcsec/pixel. For cases (ii) and (iii) the level of background is higher and they therefore require longer exposure times to reach a given S/N. In the case of R = 1000, this is compensated by the greater number of galaxies that can be observed. However for R = 100, the increased incidence of overlap is not compensated by the potential multiplex gain.

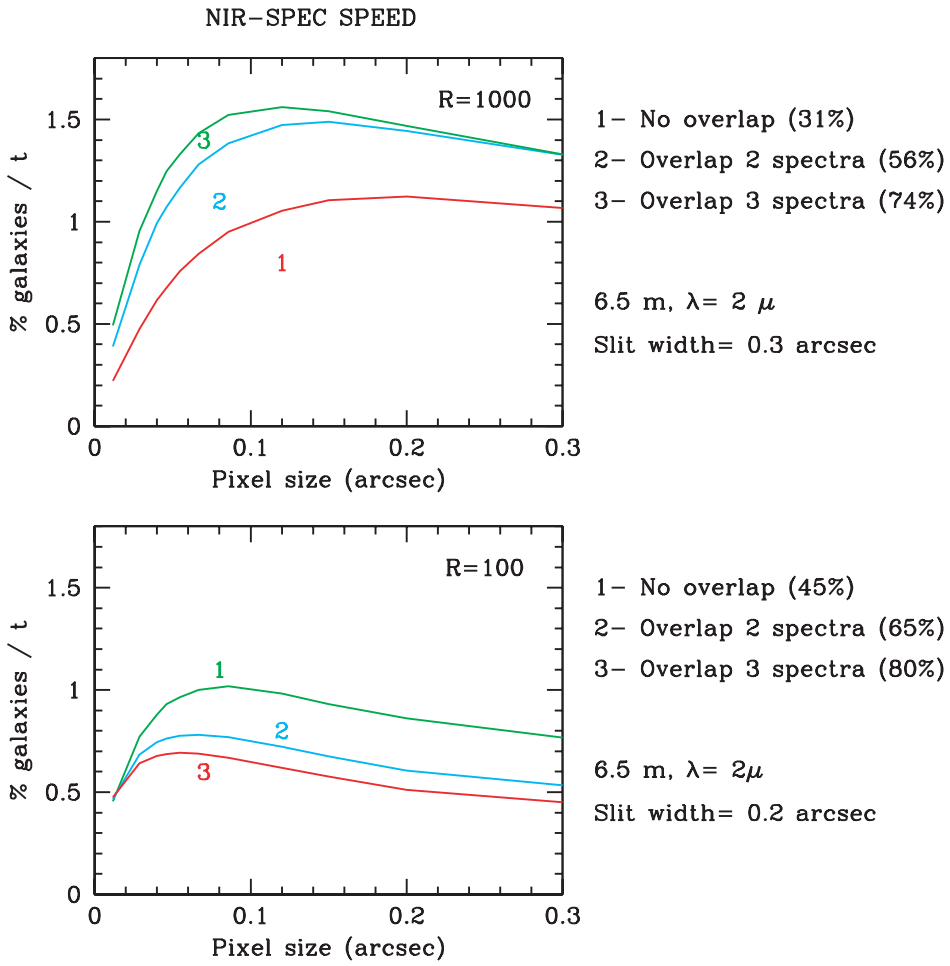

Figure 6: Speed of the spectrograph as a function of the pixel scale for three cases: (i) no overlap allowed, (ii) overlap of two spectra is allowed and (iii) overlap of three spectra is allowed. The speeds are normalized to the value corresponding to 'no overlap' for scale = 0.1 arcsec/pixel. For cases (ii) and (iii) the level of the background is higher (see figure 5), and therefore requires longer exposure times to reach a given S/N, but this is compensated, at R = 1000, by the fact that more galaxies are observed. This is not the case for R = 100, for which a sequential procedure is more efficient.

In summary, the conclusions from the results in Figure 6 are:

- ❏ For R = 1000 and multi-object observations, the scale which maximises global efficiency 'speed' is somewhat smaller (~ 0.1 arcsec/pixel) than the one which maximises sensitivity (~ 0.16 arcsec/pixel).
- ❏ For R = 1000, a scale of 0.05 arcsec/pixel implies a loss in speed of about 30% with respect to the one for 0.1 arcsec/pixel.
- ❏ For R = 1000, multi-object observations are more efficient when allowing the overlap of 2 or 3 spectra.
- ❏ For R = 100, multi-object observations are more efficient if done in a sequential way, i.e., without allowing spectra overlap.

6. Facets

Since a slit is built up from a small sub-array of facets, the facet size should be always equal to or smaller than the desired slit. On the other hand, the larger the facet, the smaller the array of facets needed to cover a certain FOV, and the smaller diffraction and inter-facet losses.

So far, the number of facets in a MEMS array has been considered to be tied to the number of pixels at the detector through a 1–1 or 1–2 projection. However, there is no explicit reason for that. Just the contrary: previous sections indicate that, for relatively small pixels, the observations will be closer to a detector limited regime which implies that the slits can be larger in both length and width which relaxes the requirements for the number and size of the MEMS facets: they can be fewer and larger, especially for R = 1000.

Another conclusion is that the two dimensions of the facets do not play the same role. While the dimension along the dispersion direction is important to select the slit width, the facet dimension along the spatial direction can be relaxed and it could be larger than considered so far in the yardstick design (e.g., 0.2 arcsec or larger), which would reduce the number of facets as well as diffraction and interfacet losses. [*Note that longer facets along the spatial direction do not imply a loss in spatial (or spectral) resolution*]. They do, however, imply a loss in flexibility when configuring a multi-object mask. For the expected density of objects (~100–200 objects /arcmin^2), a factor of 2 or 3 longer spatially than spectrally would not adversely affect the global performance of the spectrograph.

Regarding the dimension along the spectral direction, values of 0.1 arcsec seem reasonable provided that R = 100 requires slit widths of the order of 0.2 arcsec. However, if the R100 mode is ultimately implemented in the NIR camera, and NIRSpec is restricted to R1000 for programmes like DRM15 (i.e., 'point' sources in a detector limited regime), the requirements for the MEMS dimensions can be relaxed even more (i.e., ~ 0.15 arcsec × 0.3 arcsec, or larger).

7. Conclusions

For the assumptions employed throughout this note we conclude:

1 Pixel Scale

At the detector, a scale of 0.1 arcsec/pixel appears to be the best option since:

- ❏ it maximises sensitivity and speed for R = 100,
- ❏ it maximises speed for R = 1000, and
- ❏ it gives more than 90% of maximum sensitivity for R = 1000. A scale of 0.05 arcsec/pixel gives a nearly optimum sensitivity and speed for R = 100, but it implies substantial losses in sensitivity and speed for R = 1000 (exposure times longer by 30–40%).

2 Slit dimensions

R = 1000. For obsevations of (nearly) point objects in a detector limited regime, slit widths as large as 0.3–0.4 arcsec optimise S/N. However, smaller slit widths give lower zodiacal background and, in dense fields, reduce crowding effects which increases the overall speed of the spectrograph.

For R = 100 and DRM15-like observations, slit widths of about 0.2 arcsec optimise S/N. In crowded fields, a sequential procedure (i.e., without allowing spectral overlap) is generally faster.

3 Facet dimensions

The two orthogonal dimensions of the MEMS facets do not play the same role.

Along the spatial direction the facet dimension could be larger than considered so far (e.g., 0.2 arcsec or larger) which would reduce the number of MEMS facets for a given FoV as well as the diffraction and interfacet losses. Note that this does not imply a loss in spatial or spectral resolution. The disadvantage of larger facets is a loss in flexibility when configuring a multi-object mask. However, for the expected density of objects (~100 objects/arcmin^2) a factor 2 or 3 larger than in the yardstick design should not have a significant negative impact on the global performance of the instrument.

Regarding the dimension along the spectral direction, values of 0.1 arcsec are reasonable provided that R = 100 requires slit widths of ~ 0.2 arcsec.

Final remark

The present analysis is based on a rather optimistic assumption about detector performance, i.e., a dark current of 0.02 e^-/s as the major contributor to the detector noise. If sensitivity/speed are the main drivers when optimising the performace of the spectrograph, a reduced detector peformance (higher dark current) implies that the pixel scale should be somewhat larger. However, the present results show that there is a relatively generous range of acceptable values and larger pixels would compromise the spatial resolution.

In any case, updated PSF profiles and detector characteristics may suggest a further refinement of the present analysis.

Acknowledgements: Thanks to John Trauger, Larry Petro and Mauro Giavalisco who provided the NGST-PSFs, ETC information, and updated values for the zodiacal light, respectively.

References

Bely, P. et al. 2001, NGST-Monograph No. 7
http://www.ngst.nasa.gov/public/unconfigured/doc_0791/rev_04/ monograph7_v10.pdf

Gardner, J. P. et al. 2000, AJ, 2000, 119, 486

Horne, K. 1988, PASP, 98, 609

Petro, L. & Stockman, H.S. 2000,
http://www.ngst.stsci.edu/nms/main/docs.html

Pirzkal et al. 2001, A&A, 375, 351

Samsom, R. & Petro, L. 2000,
http://www.ngst.stsci.edu/nms/main/nms_etc_form.html